Continued-fraction approximants to spin correlation functions. Application to NMR line shapes*

M. Engelsberg and Nai-Cheng Chao
Departamento de Física, Universidade Federal de Pernambuco, 50.000 Recife, Pe., Brazil
(Received 10 June 1975)

A simple decoupling procedure for the equations of motion of the Green's function relevant to the NMR-line-shape problem is proposed. Explicit formulas are presented for approximants to the line shape incorporating the exact values of several moments. In CaF_2 the approximants containing the second through eighth moments are found to be in very good agreement with the experimental ^{19}F free-induction-decay signals. Excellent agreement is also found between the approximants containing the second through sixth moments and the exchange-narrowed ^{19}F line shapes in paramagnetic MnF_2, $RbMnF_3$, and $KMnF_3$.

I. INTRODUCTION

Since the pioneering work of Van Vleck[1] the interpretation of NMR line shapes in solids has attracted considerable attention. Although the relevant nuclear-spin Hamiltonians that describe the interactions between nuclear spins in real systems are often known to a considerable degree of accuracy, the agreement between calculated profiles and experimentally observed line shapes has not always been completely satisfactory.

Since the many-body character of the nuclear-spin Hamiltonian makes exact line-shape calculations in real systems unfeasible, some type of approximation must always be employed. Several approximate techniques,[2-6] sometimes of rather general applicability, have been used in the calculation of NMR line shapes with various degrees of success. Unlike the line shape, its moments can be calculated exactly. Such calculations, however, become increasingly difficult as the order of moment increases. In practice only a few lowest-order moments can be expected to be known exactly in three-dimensional systems. Moreover, these moments can often but not always be determined experimentally with accuracy from the measured line shapes.

The knowledge of the exact value of only a few moments is by itself not sufficient however, to describe the details of experimentally observed line shapes. In spite of this, model functions with a few adjustable parameters are known to exist,[7,8] which fit various experimental line shapes quite well provided the parameters are adjusted to yield the correct values of a few of the lowest moments. However, the choice of these model functions that fit some experimental line shapes has frequently been rather arbitrary and somewhat mysterious. In this paper we present a technique for systematically generating approximants to NMR line shapes based upon the knowledge of the exact values of a few of its moments. Starting with the exact set of equations for the Green's functions of the system, we make a transformation that allows us to express the relevant Green's function in the form of a continued-fraction expansion. A decoupling procedure is introduced which involves an assumption about the limiting behavior of some functions of the higher moments. Although the precise conditions for the validity of this assumption are not investigated, it appears to yield correct results for widely different systems of nuclear spins.

Two types of experimentally determined line shapes were adopted as a test of the validity of the assumptions made and of the accuracy of the resulting approximants: The ^{19}F free-induction-decay signals (FID) in CaF_2 (related to the line shape by a Fourier transformation) and the exchange-narrowed ^{19}F line shapes in paramagnetic systems of the type of MnF_2. In both cases the calculated approximants are in excellent agreement with the experimental results.

Slightly different approximants,[9] of which the present ones are a generalization, were known to describe quite well the FID signals in CaF_2. Our more general approximants, which include values of the totality of the known moments in all cases, yield in addition, truncated Lorentzian-like line shapes in the exchange-narrowed systems. These profiles and the resulting line widths are also in excellent agreement with the experimental results in the paramagnetic systems.

II. GREEN'S-FUNCTION APPROACH TO THE LINE-SHAPE PROBLEM

A. Hamiltonians

The systems to be studied can be considered as being a rigid lattice of nuclear spins in a static field $\vec{H}_0$ applied along the z axis of a rectangular coordinate system. The spins are also irradiated by a rotating magnetic field of small amplitude H_r perpendicular to $\vec{H}_0$ and rotating at angular

frequency ω.

The total Hamiltonian $\mathcal{H}$ for the system can be written as the sum of three terms:

$$\mathcal{H} = \mathcal{H}_0 + \mathcal{H}_r + \mathcal{H}_1 , \quad (1)$$

$$\mathcal{H}' = \mathcal{H}_0 + \mathcal{H}_1 ,$$

where $\mathcal{H}_0 = -\gamma H_0 \sum_j I_{jz}$ is the Zeeman energy (in frequency units) of the nuclear spins of gyromagnetic ratio γ in the static field H_0.

The interaction energy of the nuclear magnetic moments with the radio-frequency field has the form

$$\mathcal{H}_r = -\tfrac{1}{2}\gamma H_r (I_+ e^{i\omega t} + I_- e^{-i\omega t}) , \quad (2)$$

where $I_\pm$ are the usual raising and lowering spin angular momentum operators.

The term $\mathcal{H}_1$ in Eq. (1) represents the mutual coupling energy of the nuclear spins and, possibly, the energy of interaction with electronic spins. We will confine this discussion to two types of interaction Hamiltonians of practical importance. The first type describes a system of nuclear spins interacting via their magnetic dipole-dipole moments only. If this interaction is only a small perturbation of the Zeeman energy, the relevant Hamiltonian $\mathcal{H}_1^d$ is a truncated[7] dipolar Hamiltonian of the form

$$\mathcal{H}_1^d = \sum_{i>j} D_{ij} (\vec{I}_i \cdot \vec{I}_j - 3 I_{iz} I_{jz}) . \quad (3)$$

The dipolar coupling constant D_{ij} is given by

$$D_{ij} = \tfrac{1}{2}\gamma^2 \hbar (3\cos^2\theta_{ij} - 1)/r_{ij}^3 ,$$

where r_{ij} is the length of the internuclear vector and θ_{ij} is the angle between $\vec{r}_{ij}$ and the static field $\vec{H}_0$.

In CaF_2 the ^{19}F spins form a simple cubic lattice of spin-$\frac{1}{2}$ nuclei coupled by magnetic dipole-dipole interactions, and the Hamiltonian $\mathcal{H}_1^d$ of Eq. (3) adequately describes the system. Using this Hamiltonian, the second through eighth moments have been calculated.[1,10] These moments are in very good agreement with the experimental values[11] that can be determined accurately in CaF_2.

The second type of system is characterized by an interaction Hamiltonian of the form

$$\mathcal{H}_1^p = \mathcal{H}_h + \mathcal{H}_e$$

$$= \sum_{ij} \sum_{\nu} A_{ij}^{\nu\nu} I_{i\nu} S_{j\nu} + \sum_{l>m} J_{lm} \vec{S}_l \cdot \vec{S}_m , \quad (4)$$

with $\nu = x, y, z$.

The first term $\mathcal{H}_h$ in Eq. (4) represents the hyperfine coupling between the nuclear magnetic moments (spins I) and the electronic magnetic moment of magnetic ions (spins S). The static field $\vec{H}_0$ along the z axis is assumed to be parallel to a principal axis of the hyperfine tensor $\vec{A}_{ij}$. The second term $\mathcal{H}_e$ in Eq. (4) represents an isotropic exchange interaction between the electronic spins.

The Hamiltonian $\mathcal{H}_1^p$ in Eq. (4) adequately describes the dominant interactions experienced by the ^{19}F spins in paramagnetic systems of the MnF_2 type where the following conditions are met: (a) Interactions involving nuclear magnetic moments can be neglected compared to interactions involving electronic spins. (b) The simple form adopted for the exchange Hamiltonian is valid because Mn^{++} is an orbital singlet and terms representing crystal-field effects are small.

Experimentally determined[12] ^{19}F line shapes in paramagnetic MnF_2 and also $RbMnF_3$ and $KMnF_3$ are Lorentzian-like over the experimentally observable range. Thus, the moments of these line shapes cannot be measured since they are determined almost exclusively by the behavior of the unobservable wings of the resonance. However, the second, fourth, and sixth moments have been calculated[8] using the Hamiltonian $\mathcal{H}_1^p$ of Eq. (4) together with experimental values for the exchange and hyperfine interactions that are quite accurately known in these materials.

For the paramagnetic systems considered here, the exchange interaction J in Eq. (4) is much larger than the Zeeman energy in a field of the order of 10^4 G. The hyperfine interaction A, however, can be considered as a small perturbation of the Zeeman energy in the same fields. These relationships

$$J \gg \gamma H_0 \gg A \quad (5)$$

will be repeatedly invoked.

B. Linear-response theory

The formalism of the Green's function[13,14] will be used to derive[15] an expression for the rf susceptibility that determines the NMR line shape.

Starting with a density matrix ρ whose initial thermal-equilibrium value is given by

$$\rho(0) = e^{-\beta\mathcal{H}'}/\mathrm{Tr}(e^{-\beta\mathcal{H}'}) , \quad (6)$$

where $\beta = \hbar/kT$, one defines a transformed density matrix

$$\rho^* = e^{i\mathcal{H}'t} \rho e^{-i\mathcal{H}'t} .$$

$\mathcal{H}' = \mathcal{H}_0 + \mathcal{H}_1$ is the Hamiltonian in the absence of rf irradiation [Eqs. (1)–(4)].

Under the influence of the total Hamiltonian $\mathcal{H} = \mathcal{H}_r + \mathcal{H}'$, the equation of motion of the density matrix ρ has the form[7]

$$\frac{d\rho}{dt} = i[\rho, \mathcal{H}] . \tag{7}$$

The time-evolution of the transformed density matrix ρ^* can be obtained from Eq. (2) and (7). The result is

$$\frac{d\rho^*}{dt} = -\tfrac{1}{2} i \gamma H_r [\rho^*, \{I_+(t)e^{i\omega t} + I_-(t)e^{-i\omega t}\}] , \tag{8}$$

where

$$I_\pm(t) = e^{i\mathcal{H}'t} I_\pm e^{-i\mathcal{H}'t} .$$

The linear response of the system to a small perturbing rf field is obtained by neglecting terms in H_r of higher order than the first in the iterative integration of Eq. (8). After transforming back to the laboratory frame the result for $\rho(t)$ is

$$\rho(t) = \rho(0) - (\tfrac{1}{2} i H_r \gamma) \int_{-\infty}^{t} [\rho(0), (e^{i\mathcal{H}'(\tau-t)} I_+ e^{-i\mathcal{H}'(\tau-t)} e^{i\omega\tau} + e^{i\mathcal{H}'(\tau-t)} I_- e^{i\mathcal{H}'(\tau-t)} e^{-i\omega\tau})] \, d\tau , \tag{9}$$

where $\rho(-\infty) = \rho(0) = \rho^*(-\infty)$.

The quantity of interest in a cw NMR experiment is the component of magnetization transverse to the static field $\vec{H}_0$ produced by a transverse magnetic field rotating with angular velocity ω. This can be specified by the expectation value of the operator I_+,

$$\bar{I}_+(t) = \mathrm{Tr}[\rho(t) I_+] . \tag{10}$$

We will use angular brackets to denote thermal-equilibrium expectation values:

$$\langle Q \rangle = \mathrm{Tr}[\rho(0) Q] .$$

In the high-temperature approximation appropriate to the present experimental conditions, the thermal-equilibrium density matrix has a spin-dependent part of the form

$$\rho(0) = -\beta \mathcal{H}' / \mathrm{Tr}(1) . \tag{11}$$

Since $\mathrm{Tr}[\rho(0) I_+] = 0$, Eqs. (10) and (9) yield the following expression for $\bar{I}_+(t)$:

$$\bar{I}_+(t) = \frac{i H_r \gamma}{2} \int_{-\infty}^{t} \mathrm{Tr}\{I_-[\rho(0), I_+(t-\tau)]\} e^{-i\omega\tau} d\tau . \tag{12}$$

Implicit in Eq. (12) is the vanishing value of the term $\langle [I_+(\tau - t), I_+] \rangle$ in the high-temperature approximation.

Examination of this trace confirms this result for $\mathcal{H}_1^d$ of Eq. (3) and also for $\mathcal{H}_1^p$ of Eq. (4) in the crystals to be considered.

Introducing a step function $\Theta(t)$,

$$\Theta(t) = 0 , \quad t < 0$$

$$\Theta(t) = 1 , \quad t > 0$$

one can obtain a useful expression for the complex rf susceptibility $\chi(\omega)$:

$$\bar{I}_+(t) = (\tfrac{1}{2} i H_r \gamma) e^{-i\omega t} \int_{-\infty}^{\infty} \Theta(t') \langle [I_+(t'), I_-] \rangle e^{i\omega t'} dt'$$

$$= H_r e^{-i\omega t} \chi(\omega) . \tag{13}$$

In order to insure convergence of the integral of Eq. (13) a convergence factor $e^{-\epsilon t}$ ($\epsilon > 0$) is introduced into the integrand yielding the following expression for $\chi(\omega)$:

$$\chi(\omega) = \lim_{\epsilon \to 0} i\gamma\pi \, \langle\langle I_+, I_- \rangle\rangle_{\omega + i\epsilon} , \tag{14}$$

where

$$\langle\langle I_+(t), I_- \rangle\rangle = \Theta(t) \langle [I_+(t), I_-] \rangle \tag{15}$$

is the retarded double-time Green's function and $\langle\langle I_+, I_- \rangle\rangle_{\omega + i\epsilon}$ is its Fourier transform given by

$$\langle\langle I_+, I_- \rangle\rangle_{\omega + i\epsilon} = \frac{1}{2\pi} \int_{-\infty}^{\infty} e^{i(\omega + i\epsilon)t'} \langle\langle I_+(t'), I_- \rangle\rangle \, dt' . \tag{16}$$

The line shape is associated with the absorption of energy from the rf field and is determined by the imaginary part of the complex rf susceptibility $\chi(\omega)$ specified by Eq. (14).

C. Equations of motion

The equations of motion for the Green's function are obtained by taking the time derivative of both sides of Eq. (15) followed by a Fourier transformation [Eq. (16)]. The left-hand side of Eq. (15) is then integrated by parts yielding

$$(\omega + i\epsilon) \langle\langle I_+, I_- \rangle\rangle_{\omega + i\epsilon}$$

$$= (i/2\pi) \langle [I_+, I_-] \rangle + \langle\langle [I_+, \mathcal{H}'], I_- \rangle\rangle_{\omega + i\epsilon} . \tag{17}$$

By substituting $\mathcal{H}' = \mathcal{H}_0 + \mathcal{H}_1$ into the term $\langle\langle [I_+, \mathcal{H}'], I_- \rangle\rangle_{\omega + i\epsilon}$, Eq. (17) can be further simplified yielding

$$(\Omega + i\epsilon) \langle\langle I_+, I_- \rangle\rangle_{\omega + i\epsilon} = (i/2\pi) \langle [I_+, I_-] \rangle + \langle\langle [I_+, \mathcal{H}_1], I_- \rangle\rangle_{\omega + i\epsilon} , \tag{18}$$

where $\Omega = \omega - \gamma H_0$.

Iteration of Eq. (18) yields a hierarchy of Green's functions $G_n(\Omega + i\epsilon)$ of various orders n. The equations of motion have the form

$$
\begin{aligned}
(\Omega + i\epsilon)G_0 &= (i/2\pi)C_0 + G_1, \\
(\Omega + i\epsilon)G_1 &= (i/2\pi)C_1 + G_2, \\
&\vdots \qquad\qquad \vdots \\
(\Omega + i\epsilon)G_n &= (i/2\pi)C_n + G_{n+1}, \\
&\vdots \qquad\qquad \vdots
\end{aligned}
\tag{19}
$$

where

$$G_n(\Omega + i\epsilon) = \langle\langle [I_+, \mathcal{H}_1]_n, I_- \rangle\rangle_{\omega + i\epsilon}$$

and $[I_+, \mathcal{H}_1]_n$ denotes the n-fold commutator

$$[[[\ldots[I_+, \mathcal{H}_1], \mathcal{H}_1], \mathcal{H}_1] \ldots \mathcal{H}_1].$$

In the same manner $C_n = \langle [[I_+, \mathcal{H}_1]_n, I_-] \rangle$.

It is clear from Eqs. (19) that the Green's function $G_0(\Omega + i\epsilon)$ and hence the line shape, is determined by the values of the constants $C_n = \langle [[I_+, \mathcal{H}_1]_n, I_-] \rangle$. Examination of the thermal-equilibrium averages determining the values of the parameters C_n in the dipolar case (i.e., $\mathcal{H}_1 = \mathcal{H}_1^d$) shows[15] that they are proportional to the central moments of the line shape. This can also be shown to hold in the paramagnetic systems (i.e., $\mathcal{H}_1 = \mathcal{H}_1^p$) provided $\gamma H_0 \gg A$. Since this condition is satisfied for the paramagnetic systems considered here, one has in both the dipolar and paramagnetic systems

$$C_n = b M_n, \tag{20}$$

where b is a proportionality constant and M_n are central moments of the line shape given by[7]

$$M_n = \mathrm{Tr}([\mathcal{H}_1[\mathcal{H}_1[\mathcal{H}_1 \ldots [\mathcal{H}_1, I_x]]] \ldots] I_x) / \mathrm{Tr}(I_x^2). \tag{21}$$

In the paramagnetic systems MnF_2, $RbMnF_3$, and $KMnF_3$, the NMR central moments of the ^{19}F line shapes have been calculated[8] keeping only the leading terms in Eq. (21). Since the exchange interaction J is much larger than the hyperfine interaction A, terms in the nth moment of higher order in A than $A^2 J^{n-2}$ were neglected.

For the systems of interest $C_n = 0$ for n odd. Defining renormalized Green's functions g_n by

$$
\begin{aligned}
g_n &= i(2\pi/b)G_n \quad (n \text{ odd}), \\
g_n &= (2\pi/b)G_n \quad (n \text{ even}),
\end{aligned}
$$

Eqs. (19) take the form

$$
\begin{aligned}
S g_0(S) &= 1 - g_1(S), \\
S g_1(S) &= g_2(S), \\
S g_2(S) &= M_2 - g_3(S), \\
S g_3(S) &= g_4(S), \\
S g_4(S) &= M_4 - g_5(S), \\
&\vdots \qquad\qquad \vdots
\end{aligned}
\tag{22}
$$

where $S = \epsilon - i\Omega$.

The correlations of interest in the NMR case are contained in the zeroth-order Green's function $g_0(S)$. Although all the moments M_n are coupled to $g_0(S)$ through Eqs. (22), it will be possible to use the information contained in only a few of the lowest moments together with a suitable decoupling procedure to describe a variety of experimentally observed line shapes.

D. Decoupling

We assert that in real many-body systems, it is possible to construct from the sequence of moments $\{M_n\}$ subsequences $\{\tau_n\}$ that converge to a finite limit. This statement forms the basis of the proposed decoupling procedure. It will become apparent that for the systems considered here, the convergence of these subsequences is fast enough to yield good approximants from the knowledge of only a few moments.

The quantities $\{\tau_n\}$ are introduced in the following manner[9]:

$$
\begin{aligned}
\tau_{2n}^{-1} &= \left(\frac{\nu_{2n-1}^2 \nu_{2n-3}^2 \cdots \nu_1^2}{\nu_{2n-2}^2 \nu_{2n-4}^2 \cdots \nu_0^2} \right) |\nu_0|, \\
\tau_{2n+1}^{-1} &= \left(\frac{\nu_{2n}^2 \nu_{2n-2}^2 \cdots \nu_2^2}{\nu_{2n-1}^2 \nu_{2n-3}^2 \cdots \nu_1^2} \right) |\nu_0|, \quad n = 1, 2, 3 \cdots
\end{aligned}
\tag{23}
$$

with

$$\tau_0^{-1} = \tau_1^{-1} = (M_2)^{1/2} = |\nu_0|.$$

The parameters ν_n in Eq. (23) which are assumed to be nonzero[9] are functions of the moments of the form[16]

$$\nu_j^2 = D_{j-1} D_{j+1} / D_j^2, \tag{24}$$

where D_j is the following determinant:

$$
D_j = \begin{vmatrix}
1 & 0 & M_2 & \cdots & M_j \\
0 & M_2 & 0 & \cdots & M_{j+1} \\
M_2 & 0 & M_4 & \cdots & M_{j+2} \\
0 & M_4 & 0 & \cdots & M_{j+3} \\
M_4 & 0 & M_6 & \cdots & M_{j+4} \\
\vdots & \vdots & \vdots & & \vdots \\
M_j & M_{j+1} & M_{j+2} & \cdots & M_{2j}
\end{vmatrix}
\tag{25}
$$

with $M_j = 0$ for odd values of j.

We seek a transformation of the set of Green's functions $\{g_n(S)\}$ appearing in Eqs. (22) into a set

of modified Green's functions $\{I_n(S)\}$. The desired transformation should yield equations of motion for these modified Green's functions containing only the parameters $\{\tau_n\}$ instead of the usual moments appearing in Eqs. (22).

It is found by simple substitution that with the parameters $\{\tau_n\}$ defined by Eqs. (23)–(25) the equations of motion can be written in the following symmetrical form[9]:

$$\begin{aligned} SI_0(S) &= 1 - \tau_0^{-1} I_1(S), \\ SI_1(S) &= \tau_1^{-1}[I_0(S) - I_2(S)], \\ SI_2(S) &= \tau_2^{-1}[I_1(S) - I_3(S)], \\ &\vdots \quad\quad \vdots \\ SI_n(S) &= \tau_n^{-1}[I_{n-1}(S) - I_{n+1}(S)], \\ &\vdots \\ &\vdots \end{aligned} \tag{26}$$

where the modified Green's functions $\{I_n(S)\}$ are related to the original set $\{g_n(S)\}$ by a linear transformation of the following type:

$$\begin{aligned} I_{2n+1}(S) &= \sum_{p=0}^{n} a_{2p+1}^{(2n+1)}(\tau_0\tau_1\cdots\tau_{2n}) g_{2p+1}(S), \\ I_{2n}(S) &= \sum_{p=0}^{n} a_{2p}^{(2n)}(\tau_0\tau_1\cdots\tau_{2n-1}) g_{2p}(S), \\ n &= 0, 1, 2, 3 \ldots . \end{aligned} \tag{27}$$

Since we are only interested in the zeroth-order Green's function, the exact form of the coefficients $a_l^{(m)}$ for $l \neq 0$ is not needed. These coefficients can be easily obtained, however, from Eqs. (23)–(26). For the zeroth-order Green's function one assumes $a_0^{(0)} = 1$, yielding

$$g_0(S) = I_0(S).$$

This allows us to write the following expression for the line shape:

$$\chi''(\Omega) = \lim_{\epsilon \to 0} \tfrac{1}{2} K \,\mathrm{Im}[i\gamma I_0(\epsilon - i\Omega)], \tag{28}$$

where $\Omega = \omega - \gamma H_0$.

A formal solution for $I_0(\epsilon - i\Omega)$ appearing in Eq. (28) can be obtained from Eqs. (26) in the form of a continued-fraction expansion.[17] This is most easily accomplished by defining the ratio

$$I_n(S)/I_{n-1}(S) = \lambda_{n-1}(S).$$

Substitution of the ratio $\lambda_{n-1}(S)$ into Eq. (26) yields for $n \geq 1$

$$\lambda_{n-1}(S) = \frac{1}{S\tau_n + \lambda_n(S)}, \quad n \geq 1 \tag{29}$$

for $n = 0$, Eq. (26) gives

$$I_0(S) = \frac{\tau_0}{S\tau_0 + \lambda_0(S)}. \tag{30}$$

Iteration of Eq. (29) for $n = 1, 2, 3 \cdots$ and substitution into Eq. (30) yields the following expression for the desired Green's function

$$I_0(S) = \cfrac{\tau_0}{S\tau_0 + \cfrac{1}{S\tau_1 + \cfrac{1}{S\tau_2 + \cfrac{1}{S\tau_3 + \cdots}}}} \tag{31}$$

In order to produce a decoupling in Eq. (31) the basic assumption to be made is that the two sequences $\{\tau_{2n}\}$ and $\{\tau_{2n+1}\}$ defined by Eqs. (23) tend to definite limits. These two limits need not be coincident.[9]

In practice only a few parameters $\tau_0, \tau_1, \ldots, \tau_p$ are known exactly in real systems. In accordance with our basic assumption, approximants to the line shape can be constructed by setting

$$\begin{aligned} &\tau_{p-1} = \tau_{p+1} = \tau_{p+3} = \tau_{p+5} = \cdots = \tau_{\text{limit}}, \\ &\tau_p = \tau_{p+2} = \tau_{p+4} = \tau_{p+6} = \cdots = \tau'_{\text{limit}}. \end{aligned} \tag{32}$$

The continued-fraction expansion of $I_0(S)$ [Eq. (31)] then yields for the pth-order approximant to the desired Green's function the following expression:

$$I_0^{(p)}(S) = \cfrac{\tau_0}{S\tau_0 + \cfrac{1}{S\tau_1 + \cfrac{1}{S\tau_2 + \cdots \cfrac{1}{S\tau_{p-2} + K(S)}}}}, \tag{33}$$

where

$$K(S) = \cfrac{1}{S\tau_{p-1} + \cfrac{1}{S\tau_p + K(S)}}. \tag{34}$$

Thus $K(S)$ in Eq. (34) satisfies a quadratic equation whose two roots are

$$K(S) = -\frac{S\tau_p}{2} \pm \left(\frac{(S\tau_p)^2}{4} + \frac{\tau_p}{\tau_{p-1}}\right)^{1/2}. \tag{35}$$

The two roots of $K(S)$ cause only a trivial ambiguity in the sign of $\chi_p''(\Omega)$ calculated from Eqs. (28), (33), and (35). Approximants to the line shape $\Lambda_p(\Omega) = 2\gamma\chi_p''(\Omega)/b$ corresponding to various values of p were calculated and are listed in Appendix A.

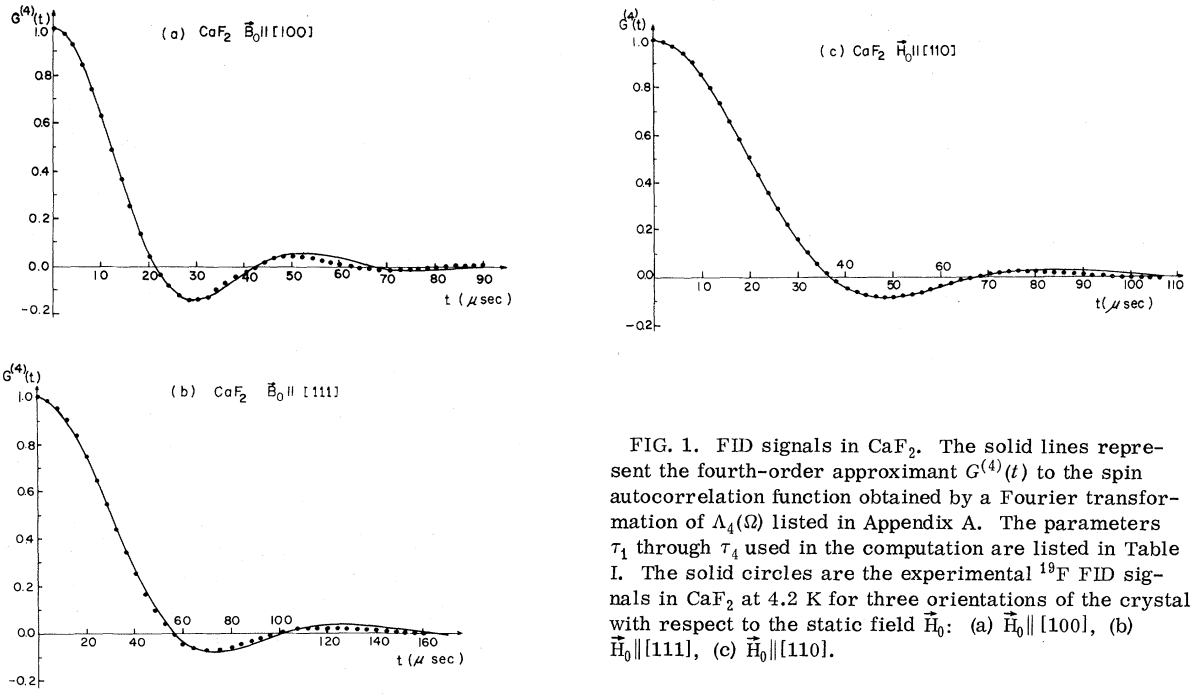

FIG. 1. FID signals in CaF_2. The solid lines represent the fourth-order approximant $G^{(4)}(t)$ to the spin autocorrelation function obtained by a Fourier transformation of $\Lambda_4(\Omega)$ listed in Appendix A. The parameters τ_1 through τ_4 used in the computation are listed in Table I. The solid circles are the experimental ^{19}F FID signals in CaF_2 at 4.2 K for three orientations of the crystal with respect to the static field $\vec{H}_0$: (a) $\vec{H}_0 \| [100]$, (b) $\vec{H}_0 \| [111]$, (c) $\vec{H}_0 \| [110]$.

III. DISCUSSION

The validity of the assumptions made in the calculation of our approximants was first tested by comparing with the experimental FID signals in CaF_2.

Figure 1 shows a plot of the Fourier transform $G^{(4)}(t)$ of the approximant $\Lambda_4(\Omega)$ listed in Appendix A together with the experimental FID signals[11] for three orientations of a CaF_2 crystal with respect to the magnetic field $\vec{H}_0$. The parameters τ_0 through τ_4 used in the computation of $\Lambda_4(\Omega)$ are listed in Table I.

The theoretical values of $(M_2)^{1/2}$ and $(M_4)^{1/4}$ were obtained from Ref. 18 and the numerical values of $(M_6)^{1/6}$ and $(M_8)^{1/8}$ were computed from Ref. 10. Since no information was available about the accuracy of the last significant figure in the

TABLE I. Parameters for ^{19}F line shape in CaF_2.

Direction of $\vec{H}_0$	n	τ_n best fit (μsec)	$(M_{2n})^{1/2n}$ (G) Best fit	Experimental [a]	Theoretical
[100]	1	11.03	3.603	3.614 ± 0.036	3.603 [b]
	2	9.82	4.349	4.352 ± 0.046	4.349 [b]
	3	7.9	4.892	4.882 ± 0.055	4.85 [c]
	4	7.9	5.338	5.326 ± 0.068	5.37 [c]
[111]	1	26.62	1.493	1.508 ± 0.019	1.493 [b]
	2	19.32	1.854	1.865 ± 0.025	1.854 [b]
	3	17.8	2.132	2.134 ± 0.028	2.11 [c]
	4	15.1	2.368	2.367 ± 0.033	2.36 [c]
[110]	1	17.92	2.218	2.191 ± 0.029	2.218 [b]
	2	14.39	2.715	2.679 ± 0.039	2.715 [b]
	3	13.95	3.070	3.026 ± 0.052	3.07 [c]
	4	12.4	3.351	3.304 ± 0.068	3.42 [c]

[a] From Ref. 11.
[b] From Ref. 18.
[c] Calculated from Ref. 10.

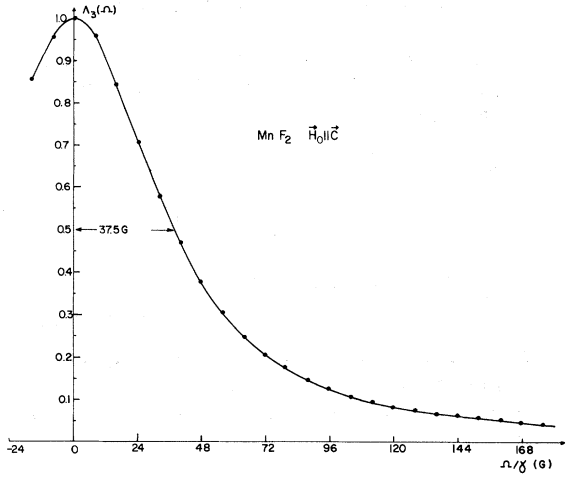

FIG. 2. ^{19}F line shape in MnF_2. The solid line represents the approximant $\Lambda_3(\Omega)$ listed in Appendix A. The parameters τ_1 through τ_3 used in the computation are listed in Table II. The solid circles represent the experimental ^{19}F line shape in MnF_2 extrapolated to infinite temperature with the static field $\vec{H}_0$ parallel to the c axis of the crystal.

computed values of $(M_6)^{1/6}$ and $(M_8)^{1/8}$, it was decided to incorporate into our approximants those values within the uncertainty of the experimental moments that yielded the best fit. The values of $(M_2)^{1/2}$, $(M_4)^{1/4}$, $(M_6)^{1/6}$, and $(M_8)^{1/8}$ adopted, the experimental values and the theoretical values are also listed in Table I for CaF_2.

It appears from Fig. 1 and the values listed in Table I that the agreement between the fourth-order approximant and the experimental FID signals in CaF_2 is very good for the three orientations of the crystal with respect to the magnetic field $\vec{H}_0$.

Figure 2 shows a similar test using the exchange-narrowed ^{19}F NMR line shape of MnF_2. A Lorentzian profile representing the experimentally observed[12] line shape and linewidth in $Mn\,^{19}F_2$ with the external magnetic field along the c crystal axis of this tetragonal crystal is shown. The experimental data correspond to the paramagnetic phase extrapolated to infinite temperature.

Also shown in Fig. 2 is the approximant $\Lambda_3(\Omega)$ appropriate to the MnF_2 case. The parameters τ_0 through τ_3 were computed from the theoretical values[8] of M_2, M_4, and M_6 and are listed in Table II for MnF_2, $RbMnF_3$, and $KMnF_3$. Also listed in Table II are the half-widths at half-height calculated from $\Lambda_3(\Omega)$ and the experimental values[12] for the three systems. For $RbMnF_3$ and $KMnF_3$ the values listed in Table II correspond to the more intense component of the doublet observed with the magnetic field along a [001] axis of these cubic crystals.

With the values listed in Table II for the parameters τ_n, the calculated profiles using $\Lambda_3(\Omega)$ are truncated Lorentzian-like functions with half-widths at half-height δ_{th} having the following simple form:

TABLE II. Parameters for ^{19}F line shape in exchange-narrowed paramagnetic crystals.

Type of crystal	n	τ_n [a] (sec)	Theoretical [b] $(M_{2n})^{1/2n}$ (G)	Experimental [c] (δ_{expt}) and calculated [d] (δ_{th}) line widths [e] (G)
MnF_2 $\vec{H}_0 \| \vec{c}$	1	$(7.93 \pm 0.08) \times 10^{-10}$	$(5.01 \pm 0.05) \times 10^4$	$\delta_{expt} = 37.2 \pm 1$
	2	$(1.53 \pm 0.08) \times 10^{-16}$	$(2.39 \pm 0.01) \times 10^6$	$\delta_{th} = 37.5 \pm 1$
	3	$(2.73 \pm 0.4) \times 10^{-10}$	$(1.09 \pm 0.01) \times 10^7$	
$RbMnF_3$ $\vec{H}_0 \| [100]$	1	$(8.9 \pm 0.3) \times 10^{-10}$	$(4.48 \pm 0.1) \times 10^4$	$\delta_{expt} = 19.7 \pm 1$
	2	$(0.49 \pm 0.2) \times 10^{-16}$	$(2.92 \pm 0.1) \times 10^6$	$\delta_{th} \approx 17$
	3	$\sim 3 \times 10^{-10}$	$(1.47 \pm 0.09) \times 10^7$	
$KMnF_3$ $\vec{H}_0 \| [100]$	1	$(8.57 \pm 0.1) \times 10^{-10}$	$(4.63 \pm 0.07) \times 10^4$	$\delta_{expt} = 19.5 \pm 1$
	2	$(0.40 \pm 0.05) \times 10^{-16}$	$(3.14 \pm 0.03) \times 10^6$	$\delta_{th} = 16.7 \pm 3$
	3	$(3.07 \pm 0.8) \times 10^{-10}$	$(1.60 \pm 0.01) \times 10^7$	

[a] Calculated from $(M_{2n})^{1/2n}$ (theoretical) and Eqs. (23)–(25) of text.
[b] From Ref. 8.
[c] From Ref. 12.
[d] From $\Lambda_3(\Omega)$ listed in Appendix A of text [$\delta_{th} = (M_2)^{1/2}(\tau_2/\tau_3)^{1/2}$].
[e] Half-widths at half-height.

$$\delta_{\rm th} = \frac{1}{\tau_1}\left(\frac{\tau_2}{\tau_3}\right)^{1/2} \approx (M_2)^{1/2}\left(\frac{M_2^2}{M_4}\right)^{1/2}\left(\frac{M_2 M_6}{M_4^2} - 1\right)^{1/2}.$$

From the results shown in Fig. 2 and Table II it appears that the agreement between the experimental line shapes and the profiles calculated from the approximant $\Lambda_3(\Omega)$ is excellent for the paramagnetic systems considered.

Thus, the simple assumption about the convergence of the parameters $\{\tau_n\}$ appears to be justified. Since the amount of computational work involved in obtaining numerical results from the approximants listed in Appendix A is small, the results are highly rewarding. Moreover, because of the general nature of the Green's-function approach and the possibility of decoupling the equations of motion in such a simple manner, it should be relatively simple to test our basic assumption for types of spin correlation functions different from the ones of interest in the NMR line-shape problem.

ACKNOWLEDGMENT

We are much indebted to Professor Bostjan Zeks of the Universidade Federal de Pernambuco for helpful discussions.

APPENDIX A: APPROXIMANTS $\Lambda_p(\Omega)$

The approximants to the line shape obtained by an application of Eqs. (33)–(35) have the following general form:

$$\Lambda_p(\Omega) = \Lambda_p(0)(1 - \tfrac{1}{4}\Omega^2\tau_p\tau_{p-1})^{1/2}/\Delta_p(\Omega) \quad \text{for } |\Omega| \leq 2/(\tau_p\tau_{p-1})^{1/2},$$

$$\Lambda_p(\Omega) = 0 \quad \text{for } |\Omega| > 2/(\tau_p\tau_{p-1})^{1/2}, \qquad \text{with } p = 1, 2, 3, \ldots \tag{A1}$$

where the denominators $\Delta_p(\Omega)$ are polynomials containing only even powers of Ω. The first four polynomials have been calculated and are listed below:

$$\Delta_1(\Omega) = 1,$$

$$\Delta_2(\Omega) = 1 + \Omega^2(\tau_1^3/\tau_2 - \tau_1^2),$$

$$\Delta_3(\Omega) = 1 + \Omega^2(\tau_1\tau_3 + \tau_1^2\tau_3/\tau_2 - 2\tau_1^2) + \Omega^4(\tau_1^4 - \tau_1^3\tau_3),$$

$$\begin{aligned}\Delta_4(\Omega) = 1 &+ \Omega^2(2\tau_1\tau_2\tau_3/\tau_4 + \tau_2^2\tau_3/\tau_4 \\ &+ \tau_1^2\tau_3/\tau_4 - \tau_1\tau_3 - \tau_2\tau_3 - 2\tau_1^2) \\ &+ \Omega^4(\tau_1^4 + 2\tau_1^2\tau_3\tau_2 + \tau_1^3\tau_3 - 2\tau_1^3\tau_3\tau_2/\tau_4 \\ &- 2\tau_1^2\tau_3\tau_2^2/\tau_4) + \Omega^6(\tau_1^4\tau_3\tau_2^2/\tau_4 - \tau_1^4\tau_3\tau_2).\end{aligned}$$

---

*Work partially supported by Banco Nacional do Desenvolvimento Econômico, Conselho Nacional de Pesquisas and CAPES (Brazilian Government).

[1]J. H. Van Vleck, Phys. Rev. 74, 1148 (1948).

[2]I. J. Lowe and R. E. Norberg, Phys. Rev. 107, 46 (1957).

[3]H. Betsuyaku, Phys. Rev. Lett. 24, 934 (1970).

[4]S. Clough and I. R. McDonald, Proc. Phys. Soc. Lond. 86, 833 (1965).

[5]W. A. B. Evans and J. G. Powles, Phys. Lett. A 24, 218 (1967).

[6]P. Borckmans and D. Walgraef, Phys. Rev. 167, 282 (1968).

[7]A. Abragam, *Principles of Nuclear Magnetism* (Clarendon, Oxford, England, 1961), Chap. 4.

[8]J. E. Gulley, Daniel Hone, D. J. Scalapino, and B. G. Silbernagel, Phys. Rev. B 1, 1020 (1970).

[9]M. Engelsberg and I. J. Lowe, Phys. Rev. B (to be published).

[10]S. J. Knack Jensen and E. Kgaersgaard Hansen, Phys. Rev. B 7, 2910 (1973).

[11]M. Engelsberg and I. J. Lowe, Phys. Rev. B 10, 822 (1974).

[12]See, for example, J. E. Gulley, B. G. Silbernagel, and V. Jaccarino, J. Appl. Phys. 40, 1318 (1969).

[13]D. N. Zubarev, Usp. Fiz. Nauk 71, 71 (1960) [Sov. Phys.— Usp. 3, 320 (1960)].

[14]D. ter Haar, *Fluctuation, Relaxation and Resonance in Magnetic Systems* (Oliver and Boyd, London, 1961).

[15]For a more detailed derivation see P. Mansfield, Phys. Rev. 151, 199 (1966).

[16]F. Lado, J. D. Memory, and G. W. Parker, Phys. Rev. B 4, 1406 (1971), and references therein.

[17]Hazime Mori, Prog. Theor. Phys. 34, 399 (1965).

[18]G. W. Canters and C. S. Johnson, Jr., J. Mag. Resonance 6, 1 (1972).